Optical Materials 107 (2020) 110067

Contents lists available at ScienceDirect

Optical Materials

journal homepage: http://www.elsevier.com/locate/optmat

Transformation of magneto-optical figure of merit for permalloy nanofilms upon oxidation

D.P. Kulikova [a,b], K.N. Afanasyev [a,c], I.V. Bykov [a,c], S.L. Efremova [a,b], A.R. Pomozov [a,b], E. E. Shalygina [b], A.V. Baryshev [a,*]

[a] Dukhov Automatics Research Institute (VNIIA), 22 ul. Sushchevskaya, Moscow, 127055, Russia
[b] Faculty of Physics, Moscow State University, 1-2 Leninskiye Gory, Moscow, 119991, Russia
[c] Institute for Theoretical and Applied Electromagnetics RAS, 13 ul. Izhorskaya, Moscow, 125412, Russia

ARTICLE INFO

Keywords:
Faraday rotation
Nanofilms
Nanostructure
Permalloy
Oxides

ABSTRACT

A series of permalloy nanofilms on glass substrates was fabricated by use of magnetron sputtering. As-deposited and thermally annealed in air oxidized nanofilms were characterized by the AFM and VSM techniques. For a temperature range of 300–475 °C, the magneto-optical figure of merit (FOM) altered in magnitude due to rise in transparency and strong change in the Faraday rotation of the oxidized nanofilms. In the near infrared range, FOM of the 425 °C-oxidized nanofilms was more than one order of magnitude larger than that of the as-deposited ones. The observed magneto-optical properties were addressed to material and structural transformations of the as-deposited nanofilms.

1. Introduction

Most of inorganic materials tend to form layers of oxides, sulfides etc. at their surfaces in air even at room temperatures [1]. For example, a silicon wafer is always covered by a native oxide layer of a few nanometers [2], the same is for metals including noble ones [3]. The material we deal with in the present work is the Ni–Fe–Mo–Mn alloy–the widespread alloy due to its unique properties (low coercive field, low magnetic anisotropy, high relative permeability, etc.); see Ref. [4] and work 10 in it for classification of Ni–Fe alloys. Long ago Ni–Fe alloys are suggested for magnetic recording technology [5] and magnetic field sensoring [6,7]. Recent works demonstrate applicability of such alloys for electromagnetic shielding [8] and biosensors [9], spintronic [10,11] and plasmonic [12] devises.

As for magneto-optical applications, Ni–Fe alloy-based plasmonic nanostructures are of continuing interest. For example, the transverse magneto-optical Kerr effect for a one-dimensional plasmonic grating is considered for local magnetic field sensoring [13,14]. Among metamaterials, the arrays of U-shaped Ni–Fe alloy scatterers are shown to exhibit the magnetization-induced circular dichroism [15]. It should be noted, however, that the magneto-optical figure-of-merit (FOM) of Ni–Fe alloys is not much attractive for designing photonic nanostructures since it is a highly absorbing material. For such application as magnetophotonic crystals [16], light absorbance in constituents is a negative issue decreasing FOM.

A number of fabrication conditions can affect the thin film micro- and nanostructure: method of sample deposition [17], pressure and temperature during fabrication [18], power density, external fields, etc. The roughness of the substrate significantly affects the magnetic film properties–the coercive field of Ni–Fe alloy film increases with the substrate roughness because of the surface-induced magnetic anisotropy [19]. Optical and magnetic properties of magnetic thin films annealed in an atmosphere significantly change [20,21]. For example, annealing samples of as-deposited garnet thin films at different temperatures leads to a growth of the Faraday rotation angle as a result of their different crystalline structure [22]. Needless to say, exact knowledge on the material parameters of a particular film is a determinant in developing functional coatings and devices on the whole.

In our work, we study island nanofilms of the Ni–Fe–Mo–Mn alloy with a thickness of ≈20 nm. Properties of the as-deposited and oxidized nanofilms (in air at 300–475 °C) were thoroughly studied. We discuss below how the initially smooth amorphous nanofilms are transformed into nanocrystalline ones upon annealing, what are the changes in their ferromagnetic, optical and magneto-optical properties.

* Corresponding author.
E-mail address: baryshev@vniia.ru (A.V. Baryshev).

https://doi.org/10.1016/j.optmat.2020.110067
Received 1 May 2020; Received in revised form 15 May 2020; Accepted 25 May 2020
Available online 22 June 2020

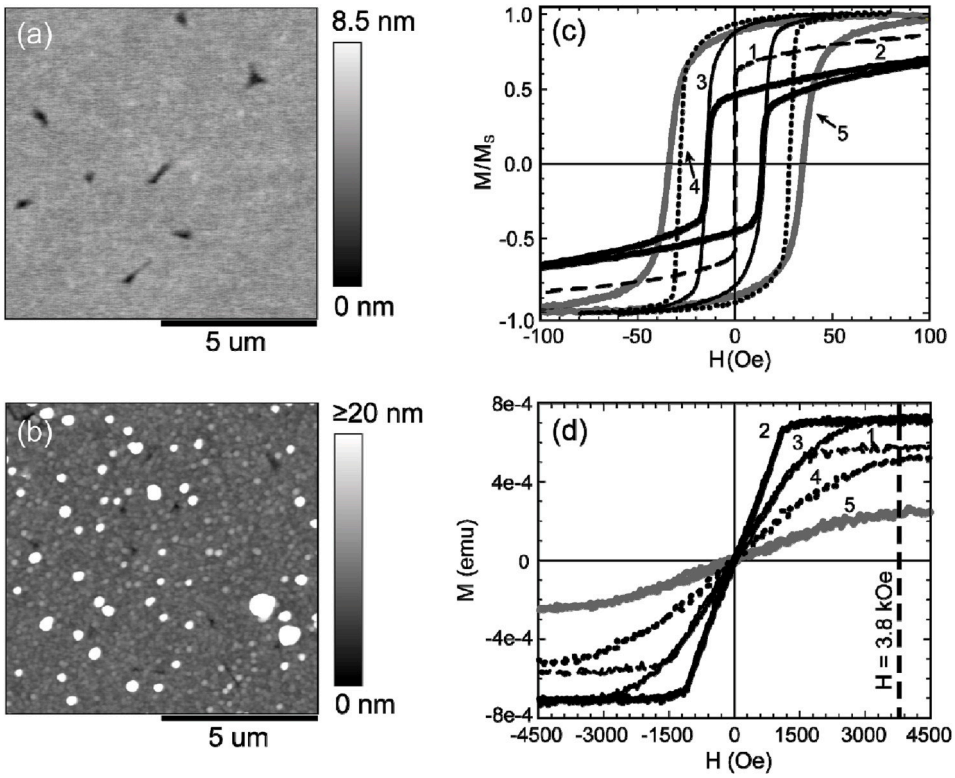

Fig. 1. (a) and (b) AFM images of a 20 nm-thick as-deposited nanofilm and an oxidized one at 450 °C. In-plane (c) and out-of-plane (d) hysteresis curves: 1–as-deposited, 2–oxidized at 300, 3–350, 4–425, 5–450 °C. Dashed line in plot (d) stands for an H-field magnitude at which the Faraday angle was measured.

2. Sample fabrication and experimental details

Island nanofilms of permalloy were deposited using magnetron sputtering from a target 79NM consisting of 78.5–80% Ni, 13.73–16.8% Fe, 3.8–4.1% Mo, 0.6–1.1% Mn, 0.3–0.5% Si, up to 0.2% Cu, up to 0.15% Ti, up to 0.15% Al, up to 0.03% C, up to 0.02% S, up to 0.02% P, according to the Russian GOST standard. The nanofilms were deposited on clean 1 mm-thick glass substrates with lateral dimensions of 10 × 10 mm. The substrates were located on a rotating holder above the target at a distance of 200 mm. The optical control at a wavelength of 600 nm was used for controlling the thickness of the as-deposited nanofilms; a control sample placed in the center of the holder was used. The vacuum chamber was pumped out to a vacuum of $5\bullet10^{-4}$ Pa. Argon was inlet by means of the gas consumption regulator to a vacuum of 0.1 Pa in the camera and was constantly pumped through a vacuum system during sputtering. The target was sputtered off at a voltage of 700 V and a current 0.5 A. The sputtering continued for about 8 min and stopped at a transmissivity of 10% for the control sample. As-deposited nanofilms were removed from the vacuum chamber and annealed in air in a temperature range of 300–475 °C for 1 h at a heating rate of 750 °C/h; we limited the temperature to prevent the substrate from melting.

Atomic force microscope (AFM) NT-MDT NTEGRA was used to investigate the surface morphology and roughness of as-deposited and oxidized nanofilms. The hysteresis loops were measured employing a Lake Shore vibrating sample magnetometer (VSM 7400). The transmission spectra of the fabricated samples were measured using a double-beam spectrophotometer Shimadzu UV-3600 Plus. Magneto-optical spectra were obtained by a home-made setup developed on the base of an J.A. Woollam V-VASE ellipsometer in a range of 500–1600 nm and an electromagnet generating magnetic fields up to $H = \pm 5$ kOe. The ellipsometric parameters Ψ and Δ represent the raw measurement from an ellipsometer–the complex ratio of $\frac{r_p}{r_s} = \tan(\Psi)\cdot e^{i\Delta}$ for the reflection coefficients of the *p*- and *s*-polarized waves and illustrate a change in polarization; Ψ stands for rotation of the polarization plane (or the main axis of the polarization ellipsis) and Δ–for evolution of the polarization state. This is why the angle of Faraday rotation (θ_F) can be determined as $\frac{\Psi(+H)-\Psi(-H)}{2}$, where $\Psi(\pm H)$ is the ratio of the amplitudes E_p/E_s measured at the opposite directions of the out-of-plane magnetic field for the transmitted light having corresponding polarizations. The parameter of Δ characterizing the phase shift between the *p*- and *s*-polarized waves was also analyzed for obtaining the magnitude of ellipticity. Note that the magneto-optical response of the initial or annealed substrates were also measured and subtracted from responses of as-deposited or oxidized nanofilms, thus obtaining their true magnitudes of θ_F.

3. Results and discussion

AFM images of a 20 nm-thick as-deposited and oxidized nanofilms are shown in Fig. 1, illustrating surface profiles before and after oxidation–smooth over ten of micron (a) and nanostructured profile (b). During annealing, the initially smooth surface of amorphous nanofilms (RMS = 1 nm) transformed into an disordered array of nanopillars having characteristic dimensions of order 45 nm × 160 nm (height × diameter) and average distance between the pillars was about 1 μm.

For the nanofims, hysteresis loops illustrate an evolution of their soft magnetic properties into harder ones; see the loops for the in-plane magnetization (Fig. 1(c)). One can see that, for the in-plane magnetization, the coercive force increased as the oxidation temperature rose and the saturation field was less than 100 Oe. As for the out-of-plane magnetization direction (Fig. 1(d)), it was the hard axis–the saturation magnetization was observed at 2 kOe for the as-deposited nanofilm, it decreased to 1 kOe in the case of 300 °C-oxidized nanofilm and again increased for the nanofilms subjected to oxidation at the higher temperatures. (The substrate had the diamagnetic type of magnetization that was subtracted from the loops). For the out-of-plane geometry, magnetization tended to its maximum for the 300-350 °C-oxidized nanofilms and dropped down at temperatures of >450 °C. The changes in magnetization behavior can be addressed to significantly increased

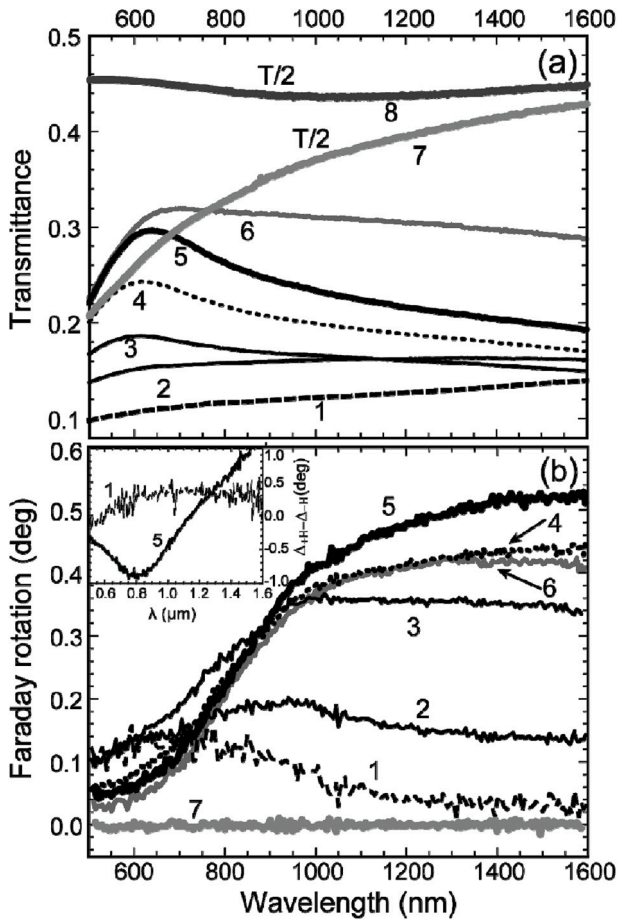

Fig. 2. (a) The transmittance and (b) the Faraday rotation spectra of fabricated nanofilms before (curve 1) and after annealing for 1 h at the series of temperatures. Curves 2–7 correspond to 300, 350, 400, 425, 450, 475 °C, and curve 8–the substrate. The inset of plot (b) shows the ellipticity difference for as-deposited and annealed at 425 °C nanofilms. Spectra 7 and 8 are divided by two. Data were collected at H = 3.8 kOe.

roughness when the as-deposited nanofilm becomes complex fragmental mixture of different in size and in crystal phase magnetic domains. Increasing number of these domains having separation between not only nanopillars but also intra-nanopillar domain walls between different oxide phases is most likely the reason for the observed hardening.

Study of optical and magneto-optical spectra showed that the oxidized permalloy nanofilms became more transparent as the annealing temperature increases. The transmittance of the sample annealed at 450 °C was about three times higher as compared with that of the as-deposited one. And, unexpectedly, the growth of θ_F in the near-infrared range was observed (Fig. 2(b)). Spectra of θ_F revealed a significant rise of the magneto-optical response for $\lambda > 800$ nm. The measured quantities of the specific Faraday rotation (degree/cm) can be compared with the ones Fe@1.0 μm-$5.1{\cdot}10^5$, Co@0.55 μm-$3.6{\cdot}10^5$ given in Ref. [23]. It is worth noting that magnitudes of specific Faraday rotation at 1.55 μm for the nanofilms under study: $0.15{\cdot}10^5$ for as-deposited and $2.6{\cdot}10^5$ for 425 °C-oxidized nanofilm. It can be seen well in Fig. 2(b) that the magnitude of θ_F was about zero for 475 °C-oxidized nanofilm. Shown in the inset ellipticity demonstrated a rise and an altering in its sign, illustrating anisotropy of polarized light coupling to nanopillars.

It is known that another important characteristic of magneto-optical materials is FOM $= \frac{\theta_F}{K}$ or $\theta_F\sqrt{T}$, where θ_F is an angle of the Faraday rotation, K–absorbance coefficient, T–transmittance of the nanofilm. FOM versus wavelength for studied samples demonstrated that oxidation at 450 °C provided larger magnitudes, see Fig. 3(a). A normalized FOM of the nanofilms for selected wavelengths versus the oxidation temperature is shown in plot (b), which is a ratio between FOM (oxidized) and FOM(as-deposited) stating more than one order of magnitude rise in the near infrared range.

To explain the observed changes in the magneto-optical response, one should take into account that recrystallization of the as-deposited nanofilms and growth of the oxide crystalline phase resulted in formation of nanopillars, which were a complex mixture of oxides NiO, Fe_2O_3, spinel $(Ni, Fe)_3O_4$, etc. [24]. Work [25] reports on nanowires fabrication and crystal phases upon oxidation of the iron foil, stating that Fe_2O_3 nanowires are better grown at 600 °C, and the Fe_3O_4 sublayers are rather thick at 400&600 °C. Previous works discussing magneto-optical and structural properties of iron oxides report that the $3d Fe^{3+}$ electrons are responsible for polarization rotation in the UV range and that, if iron is not fully oxidized, the Fe^{2+} ions in octahedral sites contribute to the rotation in the visible and near-IR ranges [[26], see also Ref. 11 in it]. The study on magneto-optical properties of $NiFe_2O_4$ spinels reports on formation of a maximum of 3 eV associated with Ni^{2+}, i.e. in the UV range [27]. Summarizing these data, one may conclude that the rise of the Faraday rotation for our samples is due to formation of Fe_3O_4 (due to Fe^{2+} ions in octahedral site) followed by oxidation up to Fe_2O_3 at temperatures > 425 °C. However, we do believe that oxidation of as-grown nanofilms containing more atoms results in a much complex nature of the found effect due to the single intervalence charge transfer transitions and intersublattice charge transfer transitions [28].

It is most likely that both the observed rise of magnetization and longer effective optical path in oxidized nanofilms are responsible for the FOM increase in the case of the nanofilms under our study. The multipass regime was used–when light bounced several times off the pair of mirrors, and thus passed repeatedly through a magnetic film situated between them–to prove the nonreciprocal behavior, thus confirming the accumulation of the polarization rotation.

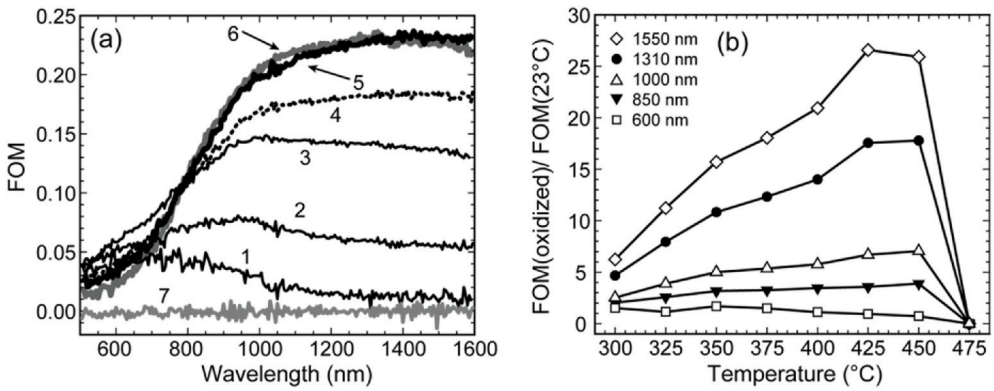

Fig. 3. (a) Changes in $FOM = \theta_F\sqrt{T}$ for the nanofilms. (b) Normalized FOM for selected wavelengths versus the oxidation temperature.

4. Conclusion

Nanofilms of permalloy subjected to oxidation in air were studied in detail. Smooth surfaces of as-deposited nanofilms were transformed into arrays of nanopillars. We demonstrate that structural and magnetic properties of oxidized nanofilms are responsible for an unusual magneto-optical response in the near infrared spectral range. For the studied series of permalloy nanofilms, we found an oxidation condition resulting in more than one order of magnitude rise of the magneto-optical figure of merit. Note also that optical properties of the fabricated films deserve special attention and will be reported elsewhere.

Declaration of competing interest

The authors declare that they have no known competing financial interests or personal relationships that could have appeared to influence the work reported in this paper.

CRediT authorship contribution statement

D.P. Kulikova: Investigation, Data curation, Writing - original draft, Writing - review & editing. **K.N. Afanasyev:** Investigation, Data curation, Writing - original draft. **I.V. Bykov:** Investigation, Data curation, Writing - original draft. **S.L. Efremova:** Investigation, Data curation, Writing - original draft. **A.R. Pomozov:** Investigation, Data curation, Writing - original draft. **E.E. Shalygina:** Investigation, Data curation, Writing - original draft, Supervision. **A.V. Baryshev:** Investigation, Data curation, Writing - original draft, Supervision, Writing - review & editing, Conceptualization.

Acknowledgments

D.P. Kulikova and A.R. Pomozov acknowledge the financial support from the Foundation for the advancement of theoretical physics and mathematics (BASIS).

References

[1] W. Henrion, M. Rebien, H. Angermann, A. Roseler, Spectroscopic investigations of hydrogen termination, oxide coverage, roughness, and surface state density of silicon during native oxidation in air, Appl. Surf. Sci. 202 (2002) 199–205, https://doi.org/10.1016/S0169-4332(02)00923-6.
[2] H. Yao, J.A. Woollam, Spectroscopic ellipsometry studies of HF treated Si (100) surfaces, Appl. Phys. Lett. 62 (25) (1993) 3324–3326, https://doi.org/10.1063/1.109059.
[3] S. Cherevko, Electrochemical dissolution of noble metals native oxides, J. Electroanal. Chem. 787 (2017) 11–13, https://doi.org/10.1016/j.jelechem.2017.01.029.
[4] C. Heck, Magnetic Materials and Their Applications, first ed., Butterworths, London, 1974.
[5] A. Chiu, I. Croll, D.E. Heim, et al., Thin-film inductive heads, IBM J. Res. Dev. 40 (3) (1996) 283–300, https://doi.org/10.1147/rd.403.0283.
[6] O. Zorlu, P. Kejik, R.S. Popovic, Structural, magnetic, and transport properties of Permalloy for spintronic experiments, Sensor. Actuator. 135 (2007) 43–49, https://doi.org/10.1063/1.3431384.
[7] A. Schuhl, F. Nguyen Van Dau, J.R. Childress, Low-field magnetic sensors based on the planar Hall effect, Appl. Phys. Lett. 66 (1995) 2751–2753, https://doi.org/10.1063/1.113697.
[8] A.V. Trukhanov, S.S. Grabchikov, A.A. Solobai, et al., AC and DC-shielding properties for the Ni80Fe20/Cu film structures, JMMM 443 (2017) 142–148, https://doi.org/10.1016/j.jmmm.2017.07.053.
[9] G.V. Kurlyandskaya, E. Fernandez, A.P. Safronov, et al., Giant magnetoimpedance biosensor for ferrogel detection: model system to evaluate properties of natural tissue, Appl. Phys. Lett. 106 (2015) 193702, https://doi.org/10.1063/1.4921224.
[10] Im Mi-Young, Hee-Sung Han, Min-Seung Jung, et al., Dynamics of the Bloch point in an asymmetric permalloy disk, Nat. Commun. 10 (2019) 593, https://doi.org/10.1038/s41467-019-08327-6.
[11] S. Iihama, Y. Sasaki, A. Sugihara, et al., Quantification of a propagating spin-wave packet created by an ultrashort laser pulse in a thin film of a magnetic metal, Phys. Rev. B 94 (2016), https://doi.org/10.1103/PhysRevB.94.020401, 020401(R).
[12] G. Armelles, L. Bergamini, N. Zabala, et al., Broad band infrared modulation using spintronicplasmonic metasurfaces, Nanophotonics 8 (10) (2019) 1847–1854, https://doi.org/10.1515/nanoph-2019-018.
[13] V.K. Belyaev, D.V. Murzin, N.N. Perova, et al., Permalloy-based magnetoplasmonic crystals for sensor applications, JMMM 482 (2019) 292–295, https://doi.org/10.1016/j.jmmm.2019.03.052.
[14] N. Kostylev, I.S. Maksymov, A.O. Adeyeye, et al., Plasmon-assisted high reflectivity and strong magneto-optical Kerr effect in permalloy gratings, Appl. Phys. Lett. 102 (2013) 121907, https://doi.org/10.1063/1.4798657.
[15] I.A. Kolmychek, I.A. Dolgikh, X. Zhou, et al., Magnetization-induced chirality in second harmonic generation response of U-shaped permalloy nanostructures, Phys. Rev. B 99 (2019), 045435, https://doi.org/10.1103/PhysRevB.99.045435.
[16] M. Inoue, M. Levy, A.V. Baryshev, Magnetophotonics: from Theory to Applications, Springer Series in Materials Science, 2013.
[17] G. Nahrwold, J.M. Scholtyssek, S. Motl-Ziegler, et al., Structural, magnetic, and transport properties of Permalloy for spintronic experiments, J. Appl. Phys. 108 (2010), 013907, https://doi.org/10.1063/1.3431384.
[18] M. Kateb, H. Hajihoseini, J.T. Gudmundsson, S. Ingvarsson, Comparison of magnetic and structural properties of permalloy Ni80Fe20 grown by dc and high power impulse magnetron sputtering, J. Phys. D Appl. Phys. 51 (2018) 285005, https://doi.org/10.1088/1361-6463/aaca11.
[19] M. Belusky, S. Lepadatu, J. Naylor, M.M. Vopson, Evidence of substrate roughness surface induced magnetic anisotropy in Ni80Fe20 flexible thin films, JMMM 478 (2019) 77–83, https://doi.org/10.1016/j.jmmm.2019.01.097.
[20] N.A. Kulesh, K.G. Balymov, V.O. Vas'kovskiy, et al., Anomalies in hysteresis properties of Fe20Ni80/Tb-Co films with unidirectional anisotropy, Thin Solid Films 577 (2017) 1–5, https://doi.org/10.1016/j.tsf.2015.01.039.
[21] A.R. Chavan, R.R. Chilwar, P.B. Kharat, K.M. Jadhav, Effect of annealing temperature on structural, morphological, optical and magnetic properties of NiFe2O4 thin films, J. Supercond. Nov. Magnetism 31 (9) (2018) 2949–2958, https://doi.org/10.1007/s10948-018-4565-3.
[22] M.-G. Kang, V.D. Quoc, S. Surabhi, et al., Spectrometer based real-time magnetic Faraday rotation spectroscopy of Bi-YIG thin films, JMMM 482 (2019) 61–65, https://doi.org/10.1016/j.jmmm.2019.03.035.
[23] A.K. Zvezdin, V.A. Kotov, Modern Magnetooptics and Magnetooptical Materials, first ed., Taylor & Francis Group, New York, 1997.
[24] Private Communication from Personnel Using the X-Ray Photoelectron Spectroscopy.
[25] Yuan Lu, Yiqian Wang, Rongsheng Cai, et al., The origin of hematite nanowire growth during the thermal oxidation of iron, Mater. Sci. Eng. B 177 (3) (2012) 327–336, https://doi.org/10.1016/j.mseb.2011.12.034.
[26] T. Tepper, F. Ilievski, C.A. Ross, et al., Magneto-optical properties of iron oxide films, J. Appl. Phys. 93 (2003) 6948, https://doi.org/10.1063/1.1540033.
[27] G.S. Krinchik, A.P. Khrebtov, A.A. Askochenskij, et al., Magneto-optical spectra of 3d ions in spinel ferrites and weak ferromagnets, Sov. Phys. JETP 45 (2) (1977) 366–372.
[28] W.F.J. Fontijn, P.J. van der Zaag, R. Metselaar, On the origin of the magneto-optical effects in Li, Mg, Ni, and Co ferrite, J. Appl. Phys. 83 (1998) 6765, https://doi.org/10.1063/1.367992.